



**HAL**  
open science

# Sulfate radical induced degradation of beta(2)-adrenoceptor agonists salbutamol and Terbutaline: Implication of halides, bicarbonate, and natural organic matter

C. Ferronato, J. Chovelon, M. Sleiman, L. Zhou, Qing Zhao, X. Wang, Claire  
Richard

## ► To cite this version:

C. Ferronato, J. Chovelon, M. Sleiman, L. Zhou, Qing Zhao, et al.. Sulfate radical induced degradation of beta(2)-adrenoceptor agonists salbutamol and Terbutaline: Implication of halides, bicarbonate, and natural organic matter. *Chemical Engineering Journal*, 2019, 368 (—), pp.252-260. 10.1016/j.cej.2019.02.183 . hal-02183217

**HAL Id: hal-02183217**

**<https://hal.science/hal-02183217v1>**

Submitted on 12 Nov 2020

**HAL** is a multi-disciplinary open access archive for the deposit and dissemination of scientific research documents, whether they are published or not. The documents may come from teaching and research institutions in France or abroad, or from public or private research centers.

L'archive ouverte pluridisciplinaire **HAL**, est destinée au dépôt et à la diffusion de documents scientifiques de niveau recherche, publiés ou non, émanant des établissements d'enseignement et de recherche français ou étrangers, des laboratoires publics ou privés.

# Sulfate radical mediated degradation of 5-halogenosalicylic acids: phenoxyl radical transformation pathways

**Lei Zhou**<sup>a, b, c\*</sup>, **Qing Zhao**<sup>a, b</sup>, **Xuerui Yang**<sup>a, b</sup>, **Corinne Ferronato**<sup>d</sup>, **Jean-Marc Chovelon**<sup>d</sup>,  
**Mohamad Sleiman**<sup>e</sup>, **Claire Richard**<sup>e\*</sup>

<sup>a</sup> Shanghai Environmental Protection Key Laboratory for Environmental Standard and Risk Management of Chemical Pollutants, School of Resources & Environmental Engineering, East China University of Science and Technology, Shanghai 200237, China

<sup>b</sup> State Environmental Protection Key Lab of Environmental Risk Assessment and Control on Chemical Processes, School of Resources & Environmental Engineering, East China University of Science and Technology, Shanghai 200237, China

<sup>c</sup> Shanghai Institute of Pollution Control and Ecological Security, Shanghai 200092, China

<sup>d</sup> Univ Lyon, Université Claude Bernard Lyon 1, CNRS, IRCELYON, F-69626, 2 Avenue Albert Einstein, Villeurbanne, France

<sup>e</sup> Université Clermont Auvergne, CNRS, Sigma-Clermont, Institut de Chimie de Clermont-Ferrand, F-63178 Aubière, France

\*Corresponding author.

Email address: [zhoulei@ecust.edu.cn](mailto:zhoulei@ecust.edu.cn) (L.Zhou); [claire.richard@uca.fr](mailto:claire.richard@uca.fr) (C. Richard)

## Abstract

In the present study, we investigated the degradation kinetics and transformation pathways of two 5-halogenosalicylic acids (5XSAs), namely, 5-chlorosalicylic acid (5CISA) and 5-bromosalicylic acid (5BrSA) by sulfate radical ( $\text{SO}_4^{\cdot-}$ ) in a thermo-activated persulfate system. The reaction pathways and mechanisms were proposed based on laser flash photolysis (LFP) techniques, HPLC-HRMS and molecular orbital calculations. Our results revealed that efficient removal of 5XSAs could be achieved by thermo-activated persulfate, and phenoxy radicals were found to play key roles in the primary oxidation pathways. The subsequent transformation of phenoxy radicals included hydroxylation and coupling processes. The resulting coupling products could undergo secondary reactions with sulfate radical, including dehalogenation, decarboxylation and hydroxylation. Hydroxylated products were in turn oxidized by  $\text{SO}_4^{\cdot-}$ , leading to the ring opening and the formation of a series of small molecular carbonyl byproducts. These processes could be responsible for the mineralization and the release of  $\text{Br}^-$  or  $\text{Cl}^-$ . In addition, the degradation rate constants of 5XSAs increased appreciably with increasing temperature, and higher efficiency of oxidation was observed around neutral initial pH. Moreover, degradation kinetics were found to be hardly affected by dissolved oxygen (DO), showing the possibility of applying SR-AOPs under environmental realistic conditions, not only for surface waters, but also for oxygen-deficient underground waters. The present work could increase our understanding of the reactivity and pathways of halogen phenols widely present in natural waters.

**Keywords:** Laser flash photolysis; Aromatic ring cleavage; Halogen release; Dissolved oxygen; Mineralization.

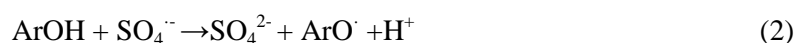
## 1. Introduction

Sulfate radical ( $\text{SO}_4^{\cdot-}$ ) based advanced oxidation processes (SR-AOPs) have attracted increasing scientific interests in recent decades for the elimination of recalcitrant contaminants from aquatic systems [1]. The half-time of  $\text{SO}_4^{\cdot-}$  is around 30-40  $\mu\text{s}$  which can react with many organic pollutants at rate constants ranging from  $10^6$  to  $10^9 \text{ M}^{-1}\text{s}^{-1}$  [2-4]. Generally, SR-AOPs are mainly based on the activation of peroxymonosulfate ( $\text{HSO}_5^-$ , PMS) or peroxydisulfate ( $\text{S}_2\text{O}_8^{2-}$ , PS) through heating [5],

UV irradiation [6, 7], ultrasound [8], adjunction of bases [9], electron [59], and transition metal-catalysis or carbons [10, 11].

Halogenated aromatic compounds have been selected as target pollutants of numerous AOPs investigations due to their widespread presence in the environment and potential toxicities towards environment and human [12-14]. Halogeno-phenols have also attracted the scientific interests because they can be introduced into the environment as chemical intermediates in the fabrication of a series of chemical products [15-17]. Degradation of halogeno-phenols by  $\text{SO}_4^{\bullet-}$  was examined in previous studies and it is well accepted that halogen release would take place. In the degradation process of 2,4,6-trichlorophenol by  $\text{SO}_4^{\bullet-}$ , Xu et al. have detected the release of chlorine atoms, which played a very important role in the subsequent formation of a series of chlorinated products [18].

As a strong electrophile,  $\text{SO}_4^{\bullet-}$  tends to react with electron-rich chemicals, including aniline and phenolic derivatives (ArOH), through an one-electron transfer reaction which was believed to be the primary pathway [19]. For example, in the case of ArOH, the initial step is an electron transfer from ArOH towards  $\text{SO}_4^{\bullet-}$  which yields an intermediate radical cation, then a spontaneous deprotonation process occurs which produces a phenoxyl radical (Eq 2) [20, 21]. On the other hand, Caregnato et al. also proposed a direct H abstraction pathway from gallic acid to  $\text{SO}_4^{\bullet-}$ , leading to the production of the corresponding phenoxyl radical and  $\text{HSO}_4^-$  [22]. In our previous study, it was documented that the formation and transformation of phenoxyl radicals played a very important role in  $\text{SO}_4^{\bullet-}$  induced oxidation of substituted phenols [23]. However, for the oxidation of halogeno-phenols by  $\text{SO}_4^{\bullet-}$ , little is currently known about the generation of corresponding phenoxyl radicals, neither on the subsequent transformation, including halogen release and mineralization.



In the present study 5-chlorosalicylic acid (5ClSA) and 5-bromosalicylic acid (5BrSA) were selected as the target chemicals, both of them are effective fungicides which have been widely applied in agriculture [58]; in addition, they can be also used as starting materials in the synthesis of pesticides, dyes and pharmaceutical products [24]. We attempted to investigate the underlying mechanisms of

**phenoxy radicals formation and its subsequent transformation pathways.** Specific objectives of this study were 1) to investigate the elementary steps in which phenoxy radicals were formed by using laser flash photolysis (LFP) experiments; 2) to identify the degradation products and propose the potential transformation pathways of phenoxy radicals; and 3) to monitor the release of halogen species from the parent chemicals.

## **2. Materials and methods.**

### **2.1. Chemicals and reagents.**

5-chlorosalicylic acid (5ClSA, 98%), 5-bromosalicylic acid (5BrSA, 98%), m-Toluic acid (mTA, 98%), potassium peroxydisulfate ( $K_2S_2O_8$ , 99%), 2,4-dinitrophenylhydrazine (DNPH, 97%), sulfuric acid ( $H_2SO_4$ , 98%), sodium hydroxide (NaOH, 98%), sodium chloride (NaCl, 99%), sodium bromide (NaBr, 99%) and orthophosphoric acid ( $H_3PO_4$ , 85%) were obtained from Sigma-Aldrich. HPLC or LC-MS grade formic acid, *t*-butanol (TBA), acetonitrile (ACN) and methanol (MeOH) were supplied by Fisher Chemical (Poole, UK). Ultrapure water (18 M $\Omega$  cm) from a Milli-Q water system (Millipore, MA, USA) was used to prepare aquatic reaction solutions and HPLC mobile phase.

### **2.2. Experiment setup.**

Degradation reactions of selected chemicals by thermo-activated PS were carried out at predetermined temperatures (30-60 °C) in a thermo-stated water bath, in screw-cap EPA vials (60 mL, amber glass, Thomas scientific) with Teflon septa. In the present study fresh PS stock solution was prepared just before each bath experiments. Specific aliquots of 5XSA and PS stock solutions were transferred to the vials to achieve a 50 mL reaction at predetermined substrate and PS concentrations. The initial pH of the reaction solutions was adjusted after the addition of PS by using NaOH (10 mM) and  $H_2SO_4$  (10 mM) to desired values. Buffer solutions were not used in this study to avoid the potential secondary reactions between  $SO_4^{\cdot-}$  and the buffer species. Prior to batch kinetic experiments, control experiments in the absence of PS or with PS at ambient temperature (i.e. 20 °C) were performed and no decrease of 5XSA concentration was observed under these conditions. During the reaction process, 0.5 mL reaction samples were withdrawn at predetermined time intervals and immediately chilled in an ice

bath to stop the oxidation. Afterwards, these samples were stored at a refrigerator (4 °C) for the analysis by HPLC-DAD, HPLC-HRMS or ion chromatography (IC) within 24 h. The identification of radicals responsible for 5XSA degradation was conducted by using TBA, a specific scavenger which reacts fast with  $\cdot\text{OH}$  while slowly with  $\text{SO}_4^{\cdot-}$  [23]. All the kinetic experiments were conducted at least in duplicate.

### **2.3 Laser Flash Photolysis (LFP).**

To record the formation and decay of the potential radicals generated during the reactions, transient absorption experiments were carried out in the time range of 0.02-500  $\mu\text{s}$ . In this work a Quanta Ray GCR 130 Nd: YAG laser and an Applied Photophysics station with laser excitation at 266 nm were used. The monitoring of transient absorption was achieved by the application of a detection system, including a pulsed xenon lamp (150 W), a monochromator and a photomultiplier. The digitized signal was analyzed by a 32 Bits RISC-processor kinetic spectrometer workstation. Prior to laser excitation, appropriate volumes of solutions containing PS and 5XSA were mixed to a desired concentrations, afterwards, approximately 3 mL reaction solution was transferred to a quartz cuvette. It is noteworthy that maximum absorption of sulfate radical in LFP was located around 450 nm, thus its formation and decay could be observed at this wavelength [26].

### **2.4. DNPH derivatization.**

DNPH derivatization method was applied in this study for the identification of carbonyl byproducts with smaller molecular weights, the procedure being similar to our previous work with some differences [24]. Specifically, 0.5 mL reaction solution was mixed with 20  $\mu\text{L}$  DNPH solution (1 mg  $\text{mL}^{-1}$  in ACN), and 20  $\mu\text{L}$  phosphoric acid (0.051 M) was used to acidify the solution. After 30 min stirring, 1 mL ACN was added, this solution was then transferred to a HPLC vial for HPLC-HRMS analysis.

### **2.5 DFT calculations.**

In the present study all the DFT calculations were conducted by using Gaussian 09 package of program, as previously documented [25, 26]. The B3LYP hybrid exchange-correlation functional was

used for geometry optimizations [27], and the basis set was set at 6-31+G(d). SMD model based on the self-consistent-reaction-field (SCRF) method was used throughout to evaluate the solvent effect of water [28]. Frequency calculations were also performed in order to confirm the natures of all minima.

## 2.6. Analyses.

The detailed analysis methods of HPLC, HPLC-HRMS and IC are described in Text S1, Supplementary Materials (SM).

## 3. Results and discussion

It is well accepted that thermolysis is an effective approach to activate PS for the generation of  $\text{SO}_4^{\cdot-}$  [1], and which was applied to the present study for 5XSA degradation. Control preliminary experiments at 60 °C without PS for 120 min revealed no loss of 5ClSA or 5BrSA, indicating that the selected target compounds were thermally stable in the experimental conditions. Additionally, 5ClSA and 5BrSA were also found to be stable in the presence of PS at ambient temperature (20 °C).

### 3.1 Reaction kinetics

#### 3.1.1 Effect of temperature.

It has often been reported that increasing temperature would markedly enhance the oxidation efficiency by thermo-activated PS [1, 38, 39]. In this study different experiments in which the temperature varying from 30 to 60 °C were tested. It was found that the degradations of 5ClSA and 5BrSA followed a pseudo-first-order kinetics (Eq 3).

$$\ln([P]/[P]_0) = -k_{obs}t \quad (3)$$

Thus, as expected the decay rate of 5ClSA and 5BrSA were appreciably increased with increasing temperature, as shown in Figure 1 (for 5BrSA in Figure S1, SM). High temperature promoted the activation of PS as well as elevated the chemical oxidations initiated by  $\text{SO}_4^{\cdot-}$  attack, which is in accordance with the literature data for other contaminants [1, 38, 39]. **Furthermore, the dependency of  $k_{obs}$  was further evaluated using the Arrhenius equation, as described in Eq. (4):**

$$\ln k_{\text{obs}} = \ln A - \frac{Ea}{RT} \quad (4)$$

where A represents the pre-exponential factor, Ea is the activation energy, R is the universal gas constant (8.314 J mol<sup>-1</sup> K<sup>-1</sup>), and T is the reaction temperature. Thus, the activation energy could be calculated as 99.7 and 85.5 kJ mol<sup>-1</sup> for 5ClSA and 5BrSA, respectively. It is noteworthy that, in the same reaction condition, the degradation of 5BrSA was faster than that of 5ClSA, this was in line with the smaller activation energy, as well as the second-order rate constants of them with SO<sub>4</sub><sup>•-</sup> by using a competitive kinetic method (Text S2, SM), and the rates were estimated at (1.04 ± 0.14) and (1.20 ± 0.11) × 10<sup>9</sup> M<sup>-1</sup> s<sup>-1</sup> for 5ClSA and 5BrSA, respectively.

### Figure 1

#### 3.1.2 Effect of initial pH

Solution pH is another important factor which plays a complex role in SR-AOPs since it can potentially affect the speciation of organic compounds with ionisable functional moieties as well as the generation of reactive species (i.e. SO<sub>4</sub><sup>•-</sup> and ·OH) [40]. Moreover, it had also been reported that SO<sub>4</sub><sup>•-</sup> can be transformed into ·OH by reactions with water and/or hydroxide ions under basic conditions (Eq 5 and 6) [41, 56], in addition, it has also been documented that in acidic conditions, SO<sub>4</sub><sup>•-</sup> can also be quenched by hydrogen ions (Eq 7) [60].

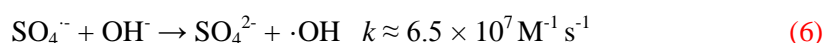
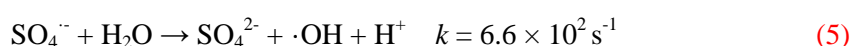
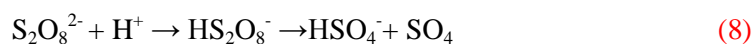


Figure 2 exhibits the impact of solution pH on 5ClSA (5BrSA) removal by thermo-activated PS at 60 °C. The most efficient degradation for both chemicals was observed at an initial pH of 7.0, increasing or decreasing the initial pH values inhibited the oxidation process. It is noteworthy that pH of reaction solutions declined continuously during the oxidation process, as no buffer was used in this work (Table S1, SM). For instance, the pH of 5ClSA reaction solutions decreased from 9.0 to 5.2, 7.0 to 4.4,



5.0 to 4.0 and 3.0 to 2.8 after 90 min. 5ClSA has two pK<sub>a</sub>s (2.59 and 12.58) [24], thus at a pH laying between 5 and 9, the dominant species is carboxylate form (5ClSA-H, Figure S2). While at pH < 5, molecular 5ClSA (protonated species) also exists. Similar speciation was also found in the case of 5BrSA, whose pK<sub>a</sub> values are 2.63 and 12.76 (Figure S3). It has been reported that the deprotonated, non-dissociated forms of phenols, tetracyclines and sulfonamides were more susceptible for SO<sub>4</sub><sup>•-</sup> attack [42, 43]. As the pH declined, the fraction of protonated 5XSA would increase, the presence of protonated 5XSA might contribute to the slower degradation at very acidic conditions (pH < 5). Moreover, in acidic conditions, PS could undergo an acid-catalyzed decomposition process which depletes PS *via* a non-radical pathway without generating SO<sub>4</sub><sup>•-</sup> (Eq 8), resulting in a lower efficiency of PS decomposition to generate SO<sub>4</sub><sup>•-</sup> [44]. Consequently, these two factors could be responsible for the weaker degradation rates at acidic pH.



In addition, the conversion of SO<sub>4</sub><sup>•-</sup> into ·OH (Eq 6 and 7) was also tested in this section by using TBA, a specific scavenger which reacts fast with ·OH (≈3.8-7.6 × 10<sup>8</sup> M<sup>-1</sup> s<sup>-1</sup>) while slowly with SO<sub>4</sub><sup>•-</sup> (≈4-9.1 × 10<sup>5</sup> M<sup>-1</sup> s<sup>-1</sup>) [23]. The presence of excess TBA (10 mM) could only slightly inhibit the degradation of 5XSA (100 μM). For instance, at initial pH of 9, the degradation rate of 5ClSA declined from 1.62 to 1.49 × 10<sup>-4</sup> s<sup>-1</sup> after TBA addition, implying that the contribution of ·OH was negligible. A similar result was also obtained for 5BrSA, the rate constant decreased from 1.61 to 1.50 × 10<sup>-4</sup> s<sup>-1</sup> after TBA addition. This result was in line with previous work that SO<sub>4</sub><sup>•-</sup> appeared as the predominant major species in activated PS process at pH < 9 [45]. Therefore, the negative effect of basic pH on 5ClSA/5BrSA degradation might be attributed to other reasons. By heat activation, one molecule of peroxydisulfate could undergo homolysis of the O-O bond to generate two SO<sub>4</sub><sup>•-</sup>, which in turn oxidizes the target pollutants (Eq 1). While at basic condition, base-activated PS decomposition could also take place (Eq 9) [9]. In this latter case, two molecules of PS only produce one molecule of SO<sub>4</sub><sup>•-</sup>, and the reaction in basic pH is therefore less efficient than that in neutral conditions.

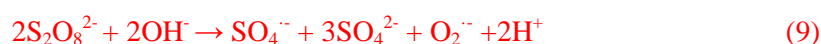


## Figure 2

### 3.2 Formation of phenoxy radicals

LFP was conducted to identify the transient species involved in the reaction between 5ClSA/5BrSA and  $\text{SO}_4^{\cdot-}$ . This technique is well appropriate because the radical  $\text{SO}_4^{\cdot-}$  formed by photochemical cleavage of PS exhibits a well-known transient spectrum ( $\lambda_{\text{max}}=450$  nm [29]) and phenoxy radicals can be also easily identified by their two-band feature transient spectrum [21] and the reaction between  $\text{SO}_4^{\cdot-}$  and the phenols can be directly monitored. In the presence of 5ClSA or 5BrSA,  $\text{SO}_4^{\cdot-}$  concentration decayed rapidly and new reactive species were formed, as it was observed for other chemicals such as salbutamol or terbutaline [23]. The new transient species generated from 5ClSA and 5BrSA ( $\lambda_{\text{max}} = 400/420$  nm and  $420/440$  nm, respectively, Figure 3A) were firmly assigned to 2-carboxy-4-chlorophenoxy radical and 2-carboxy-4-bromophenoxy radical. Indeed, these species were already observed upon laser flash photolysis of 5ClSA/5BrSA in the presence of H-donor molecules [55]. Such series of equally spaced peaks (20 nm) was attributed to the vibrational progressions of phenoxy radical, while the absorption peaks at the longer wavelength are due to the 0-0 transition, which was previously documented [20-23].

## Figure 3

To better understand the underlying pathways through which phenoxy radical was generated from the reaction of 5XSA with  $\text{SO}_4^{\cdot-}$ , DFT calculations were carried out. By considering an electron-transfer mechanism, the initial step proposed could be an addition of  $\text{SO}_4^{\cdot-}$  on the aromatic ring *via* a transition state (**TS**, Figure 3B), leading to the generation of an additional intermediate (**IM**). The structural difference between **TS** and **IM** was the different distance between sulfate radical and 5XSA (O---3C distance in Figure 3B), specifically, the distances were estimated to be 1.82 and 1.51 Å for **TS** and **IM**, respectively. The proposed sulfate addition pathway was documented in the literatures [33, 34], and such process could take place on each of the position on the ring. For sulfate addition on the 3C position on the ring (formation of **IM** *via* **TS**, Figure 3B), energy barriers of 31.8 and 30.1 kJ mol<sup>-1</sup> were calculated for 5ClSA and 5BrSA, respectively, which could be easily overcome at ambient conditions. Afterwards, **IM** could undergo cleavage to produce the corresponding phenoxy radical

and  $\text{HSO}_4^-$  (or  $\text{H}^+ + \text{SO}_4^{2-}$ ). Regarding sulfate addition on 4C, energy barriers (from **Reactants** to **TS**) at 12.1 and 9.2  $\text{kJ mol}^{-1}$  were estimated for 5ClSA and 5BrSA, respectively; and values of 19.7 and 18.0  $\text{kJ mol}^{-1}$  for 5ClSA and 5BrSA, respectively, were obtained on 6C. These relative low energy barriers corroborated the feasibility of an efficient formation of phenoxyl radical *via* an electron-transfer. On the other hand, the H abstraction process was also calculated, and calculation findings indicated that for direct H abstraction of 5XSA (OH group) by  $\text{SO}_4^{\cdot-}$  no transition state was recorded. As the energy levels of the products (phenoxyl radical and  $\text{HSO}_4^-$ ) were much lower than that of the reactants (Figure 3B), the H abstraction reactions were also thermodynamically favorable.

It is worthy to note that for electron-transfer pathway, the energy barriers (from **Reactants** to **TS**) for 5BrSA reacting with  $\text{SO}_4^{\cdot-}$  at each site on the aromatic ring was smaller than that for 5ClSA (Figure 1B), implying that 5BrSA is more susceptible to  $\text{SO}_4^{\cdot-}$  attack than 5ClSA. This result was in accordance with the degradation rates, as 5BrSA degraded faster than 5ClSA under the same condition. Both Br and Cl are regarded as electron-withdrawing groups due to the relative strong inductive effect. It is well accepted that Cl has a stronger electron-withdrawing ability than Br, leading to a lower electron density on the ring and make the electron transfer to  $\text{SO}_4^{\cdot-}$  less favorable.

### 3.3 Degradation products and oxidation pathways

#### 3.3.1 Oxidation byproducts identification

In order to construct a detailed mechanism of the 5XSA oxidation by SR-AOPs, HPLC-HRMS analysis was employed to identify the primary and secondary oxidation products generated from the reactions of 5ClSA or 5BrSA with  $\text{SO}_4^{\cdot-}$ . The presence of Cl and Br atoms were verified by their isotopic peaks of  $M/M+1.9971$  and  $M/M+1.9980$ , respectively. The MS data of 5ClSA obtained from HPLC-HRMS (in negative mode) and the proposed structures of transformation products (TPs) are listed in Table 1 (For 5BrSA in Table S2, SM).

As seen, a total of 8 primary TPs were directly identified for 5ClSA from the total ion current chromatograms (TIC) of the degradation sample. The parent compound, 5ClSA, was firstly detected at retention time (RT) of 4.41 min ( $m/z = 170.9848$  and  $172.9814$ ). At 3.99 min, a hydroxylation product

(TP1) showing  $m/z = 202.9743$  and  $204.9714$  was observed, which was formed after addition of two hydroxyl groups on the aromatic ring of 5ClISA; and the corresponding quinone product (TP2) was also identified at 3.36 min ( $m/z = 200.9587$  and  $202.9557$ ). Furthermore, a series of coupling products were detected. The product corresponding to  $m/z = 340.9622$ ,  $342.9593$  and  $344.9562$  was identified as the coupling product of 5ClISA itself (TP3), and other products including TP4-8 (Table 1) were also observed. Notably, TP7 ( $m/z = 295.0013$  and  $296.9984$ ) exhibited three different peaks in the MS chromatogram, indicating that the addition of hydroxyl groups took place at different positions on the rings. In the case of 5BrSA (Table S2, SM), similar byproducts including hydroxylation and coupling products were also identified, indicating that these two chemicals underwent similar oxidation pathways. It is noteworthy that the structures of TPs shown in Table 1 are tentatively proposed, and the information on the position of substitutions and the coupling cannot be obtained directly from the MS data.

**Table 1**

In addition, secondary carbonyl byproducts (CP) with smaller molecular weights were also detected by DNPH derivatization method (Table 2). It should be noted that for 5ClISA and 5BrSA, the identified CPs were the same. A total number of 13 CPs were observed from MS spectrum (ranging from  $C_5$  to  $C_1$ ), including one  $C_5$ , three  $C_4$ , three  $C_3$ , four  $C_2$  and two  $C_1$  CPs (detailed in Figure S4, SM). The structures in Table 2 are tentatively proposed mainly on the MS data from derivatization compound, the UV absorption around 220, 260 and 360 nm, and literature [35, 36]. Noteworthy, these CPs may have several isomers, the structures in Table 2 are one of the most possible species. These CPs were mainly generated *via* continuous oxidation after the cleavage of aromatic ring. Among them, CP1 ( $m/z = 325.0425$ ) was the largest carbonyl byproduct detected in this work, which had been already reported previously in the photolysis of 5ClISA [24]. It was also interesting to note that formaldehyde (CP13,  $m/z = 209.0312$ ) was the most abundant byproducts, while formic acid was regarded as the end-product in the extended degradation before complete mineralization.

**Table 2**

### 3.3.2 Degradation pathways

Based on the products identification mentioned above, two different oxidation pathways can be proposed (Figure 4). Under the attack by  $\text{SO}_4^{\cdot-}$ , phenoxyl radical would be initially generated, afterwards, hydroxylation and coupling pathways could take place. Hydroxylation process is a common oxidation pathway in SR-AOPs, which has been reported repeatedly in reaction of many organic contaminants, such as phenol, sulfamethazine and atenolol [19, 37]. Such process could take place *via* the reaction of the phenoxyl radicals with oxygen to give peroxy radicals. The peroxy radicals will finally lead to the generation of phenolic product [37]. It should be noted that in the present work we only detected products with 2 additional OH groups added on the ring (TP1 in Table 1), the product with one hydroxyl group was not detected, presumably due to its relative low concentration. Trihydroxylated compounds could be further oxidized or dehydrogenated to form the corresponding quinones. Afterwards, aromatic ring cleavage might take place to generate a series of smaller molecular byproducts. Moreover, with one unpaired electron, one phenoxyl radical could couple with another one to generate the dimeric compound TP3. The following oxidation processes for these dimeric chemicals included dehalogenation, decarboxylation and hydroxylation (Figure 4). For the dehalogenation process, the initial step was expected to be an electron transfer process from TP3 to  $\text{SO}_4^{\cdot-}$ , giving a radical cation and  $\text{SO}_4^{2-}$ . This radical cation was not stable, which can either undergo a deprotonation to give phenoxyl radical, or a hydrolysis process to form TP5 (Fig S6, SM), which has been confirmed by previous studies [6,13]. In addition, it was also proposed that halogen atom could be directly substituted by a hydrogen atom, resulting in the generation of TP4, similar pathway was also found in the oxidation process of triclosan, diclofenac and 2,4-dichlorophenol [13, 61, 62].

#### Figure 4

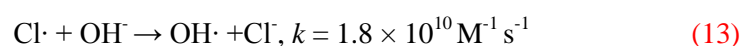
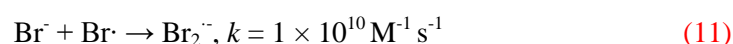
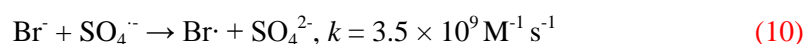
### 3.4 Mineralization and release of halogen species

Generally, oxidation of organic micro-pollutants would result in the decomposition of chemical structure and eventually lead to the mineralization into  $\text{CO}_2$  and  $\text{H}_2\text{O}$ . However, a complete mineralization of aromatic contaminant was always very difficult to achieve, mainly due to their

structure stability and antioxidant ability [49]. With  $[PS]_0 = 2 \text{ mM}$  and at  $60 \text{ }^\circ\text{C}$ , after 30 min of oxidation, approximately 25% 5ClSA was removed from the reaction system, while the decrease of TOC was found to be negligible (Figure S5); by extending the reaction time to 120 min, at which more than 75% transformation of 5ClSA was achieved, only 11% TOC removal was observed. A similar result was also obtained in the case of 5BrSA, but mineralization of 5BrSA was slightly faster than that of 5ClSA, which is in accordance with their corresponding degradation rates. TOC evolution could be due to two different pathways, the first one being the decarboxylation of the dimeric compounds as mentioned above, while the second one would result from the continuous oxidation of byproducts after ring cleavage to form  $\text{CO}_2$  and  $\text{H}_2\text{O}$ .

In addition, a dehalogenation reaction could also take place during the oxidation processes which could be proved either by the identification of byproducts in which Cl (or Br) atoms would be released or by monitoring the evolution of  $\text{Cl}^-$ ,  $\text{Br}^-$ ,  $\text{ClO}_3^-$  and  $\text{BrO}_3^-$  in solution using IC. Figure 5 shows the time-dependent evolution of  $\text{Cl}^-$  and  $\text{Br}^-$  from 5ClSA and 5BrSA during oxidation process, respectively. After 120 min of oxidation, the conversion of both 5ClSA and 5BrSA were over 90%, and free chloride ions in the reaction solution was determined at  $42.5 \text{ } \mu\text{M}$ , while  $\text{Br}^-$  was detected at  $15.1 \text{ } \mu\text{M}$ . The formation of  $\text{Cl}^-$  from 5ClSA was much more pronounced than  $\text{Br}^-$  formation from 5BrSA. Such a difference could be explained by different secondary reactions of them with  $\text{SO}_4^{\cdot-}$  [50, 51]. As mentioned above, the second-order rate constants of 5XSA with sulfate radical were estimated at  $(1.04 \pm 0.14)$  and  $(1.20 \pm 0.11) \times 10^9 \text{ M}^{-1} \text{ s}^{-1}$  for 5ClSA and 5BrSA, respectively. In addition, the reaction rate constants for  $\text{SO}_4^{\cdot-}$  with  $\text{Cl}^-/\text{Br}^-$  were also very high ( $>10^9 \text{ M}^{-1} \text{ s}^{-1}$ ), as seen in Eq 10-12. Thus, at the  $\mu\text{M}$  concentrations level, these two ions could also be oxidized by sulfate radical and lead to the formation of halogen derived oxidation products. In the case of  $\text{Br}^-$ , it would be quickly consumed by  $\text{SO}_4^{\cdot-}$  to form  $\text{Br}_2^{\cdot-}$  (Eq 10-11), a reactive bromine species, which could in turn to react with organic chemicals at a relatively high rate [26]. However, for  $\text{Cl}^-$  the secondary reactions with  $\text{SO}_4^{\cdot-}$  are completely different. In a first step, they are expected to interact with each other to yield  $\text{Cl}^\cdot$  (Eq 12). Hereafter the subsequent pathways of  $\text{Cl}^\cdot$  are complicated. It can either react with  $\text{SO}_4^{2-}$  to give back to  $\text{Cl}^-$  and  $\text{SO}_4^{\cdot-}$  (fast backward reaction of Eq 12) [50]; at  $\text{pH} > 5$  it can also react with  $\text{H}_2\text{O}$  (or  $\text{OH}^-$ )

generating hydroxyl radicals and  $\text{Cl}^\cdot$  (Eq 13) [57]. This latter process is very important for the application of SR-AOPs, as it can transform the reaction into a traditional hydroxyl radical-based reactions. The reactivity of  $\text{Cl}^\cdot$  will be highly dependent on the reaction conditions, such as pH and water matrix compositions, for instance, it can be easily scavenged by bicarbonate in natural water [57]. However, as  $\cdot\text{OH}$  played a very limited role in the oxidation process, we can conclude that reaction of Eq 13 was not important in this study, and the relative high level of free  $\text{Cl}^\cdot$  was mainly attributed to fast backwards reaction of Eq 13.



It was also reported that  $\text{Cl}^\cdot$  and  $\text{Br}^\cdot$  could ultimately be transformed to chlorate and bromate in activated persulfate system, respectively [3], for instance, the work of Lutze et al. revealed that at acidic conditions generation of  $\text{ClO}_3^-$  was favoured after the interaction of  $\text{Cl}^\cdot$  and sulfate radical [57]. However, in this work none of them was detected by IC, mainly due to their low concentrations (<1  $\mu\text{M}$ ). It is noteworthy that the presence of  $\text{Cl}^\cdot$  and  $\text{Br}^\cdot$  in SR-AOPs could also lead to the formation of Cl-DBPs and Br-DBPs, respectively, and organic pollutants might act as carbon donor during these reactions. For example, the work of Alken et al. found that  $\text{Cl}^\cdot$  could strongly interfere with dissolved organic carbon (DOC) during a SR-AOPs process, leading to the formation of chlorinated products such as chloromethane, chloroform, and methylene chloride [52]. In addition, the generation of Br-DBPs was also verified by Wang et al. in sulfate radical oxidation in the presence of natural organic matter and  $\text{Br}^\cdot$  [51]. Halogenated DBPs have been proven to cause notable risks towards environmental as well as human health [53, 54], and their formation should be taken into consideration in the application of SR-AOPs for the elimination of organic halogen pollutants.

## Figure 5

## Figure 6

### 3.5 Effect of dissolved oxygen (DO)

Recent studies revealed that DO might be involved in SR-AOPs by altering radical formation, thus affecting the degradation efficiency and pathways of organic pollutants [46, 47]. For instance, the degradation of hexachloroethane was found to be faster under anaerobic condition than aerobic condition by thermal activated PS, mainly due to the formation of  $S_2O_8^{2-}$  in the absence of oxygen [46]. SR-AOPs have widespread applications in the remediation of groundwater and surface water, the oxygen content of different water bodies differs from each other, unlike surface environments, groundwater is often oxygen-deficient. Therefore, for realistic applications of SR-AOPs, it is of great importance to evaluate the impact of DO on the oxidation efficiency of target pollutants. In the present study, 5ClSA (5BrSA) degradation by SR-AOPs was conducted under different oxygen concentrations by purging  $N_2$  and  $O_2$  into the reaction solution. As seen in Figure 6, by comparison with the control group (open to air), neither oxygen enriched nor deficient condition exhibited significant impact on 5ClSA (5BrSA) degradation, indicating that DO showed no significant effect on the transformation of corresponding phenoxy radicals which can be explained by the relatively low reactivity of phenoxy radicals towards oxygen. In most cases, it was reported that the reaction rate constants for various phenoxy radicals with  $O_2$  was ranging from  $10^4$ - $10^6$   $M^{-1} s^{-1}$ , which was much lower than the self-reactions of phenoxy radicals ( $10^7$ - $10^9$   $M^{-1} s^{-1}$ ) [48]. We propose that the impact of DO is highly dependent on the target chemicals, further study is warrant to investigate detailed mechanisms of DO involvement for each specific contaminant.

## 4. Conclusion

Thermo-activated persulfate, as one of the promising SR-AOPs, was found to be effective to eliminate 5ClSA and 5BrSA from aquatic system. The oxidation initially generated phenoxy radicals, which further underwent coupling and hydroxylation processes. Secondary reactions with sulfate radical would lead to dehalogenation, decarboxylation, hydroxylation and the aromatic ring cleavage, which were believed to be responsible for the release of halogen species ( $Br^-$  and  $Cl^-$ ) and mineralization. In addition, the degradation appeared to be highly pH-dependent and the most efficient oxidations for



both chemicals were observed at initial neutral pH. Higher temperature was beneficial to the reactions while DO exhibited no effect. The findings in the present work is of importance to reveal the underlying pathways and mechanisms of halogeno-phenols in SR-AOPs. However, practical application of SR-AOPs in water treatments needs further investigations by taking the impacts of numerous water constituents, such as dissolved organic matter and inorganic ions into consideration.

### **Acknowledgements**

The authors gratefully acknowledge the financial support from the National Natural Science Foundation of China (Grant No. 21806037).

### **Note**

Declarations of interest: none

### **References**

- [1] A. Tsitonaki, B. Petri, M. Crimi, H. Mosbæk, R.L. Siegrist, P.L. Bjerg, In situ chemical oxidation of contaminated soil and groundwater using persulfate: a review, *Crit. Rev. Env. Sci. Tec.* 40 (2010) 55-91.
- [2] W. Guo, S. Su, C. Yi, Z. Ma, Degradation of antibiotics amoxicillin by  $\text{Co}_3\text{O}_4$ - catalyzed peroxymonosulfate system, *Environ. Prog. Sustain.* 32 (2013) 193-197.
- [3] P. Neta, R.E. Huie, A.B. Ross, Rate constants for reactions of inorganic radicals in aqueous solution, *J. Phys. Chem. Ref. Data.* 17 (1988) 1027-1284.
- [4] G. Prieto, S. Beijer, M.L. Smith, M. He, Y. Au, Z. Wang, D.A. Bruce, K.P. De Jong, J.J. Spivey, P.E. De Jongh, Design and synthesis of copper–cobalt catalysts for the selective conversion of synthesis gas to ethanol and higher alcohols, *Angew. Chem. Int. Edit.* 53 (2014) 6397-6401.
- [5] Y. Fan, Y. Ji, D. Kong, J. Lu, Q. Zhou, Kinetic and mechanistic investigations of the degradation of sulfamethazine in heat-activated persulfate oxidation process, *J. Hazard. Mater.* 300 (2015) 39-47.
- [6] L. Zhou, C. Ferronato, J.-M. Chovelon, M. Sleiman, C. Richard, Investigations of diatrizoate degradation by photo-activated persulfate, *Chem. Eng. J.* 311 (2017) 28-36.

- [7] X. Liu, T. Zhang, Y. Zhou, L. Fang, Y. Shao, Degradation of atenolol by UV/peroxymonosulfate: kinetics, effect of operational parameters and mechanism, *Chemosphere*. 93 (2013) 2717-2724.
- [8] C. Cai, H. Zhang, X. Zhong, L. Hou, Ultrasound enhanced heterogeneous activation of peroxymonosulfate by a bimetallic Fe–Co/SBA-15 catalyst for the degradation of Orange II in water, *J. Hazard. Mater.* 283 (2015) 70-79.
- [9] O.S. Furman, A.L. Teel, R.J. Watts, Mechanism of base activation of persulfate, *Environ. Sci. Technol.* 44 (2010) 6423-6428.
- [10] Y.F. Huang, Y.-H. Huang, Behavioral evidence of the dominant radicals and intermediates involved in bisphenol A degradation using an efficient  $\text{Co}^{2+}$ /PMS oxidation process, *J. Hazard. Mater.* 167 (2009) 418-426.
- [11] L. Zhou, W. Zheng, Y. Ji, J. Zhang, C. Zeng, Y. Zhang, Q. Wang, X. Yang, Ferrous-activated persulfate oxidation of arsenic (III) and diuron in aquatic system, *J. Hazard. Mater.* 263 (2013) 422-430.
- [12] H. Zimmerman, *CRC Handbook of Photochemistry and Photobiology*, by W. Horspool and P.S. Song, CRC Press, London (1995) 185.
- [13] P. Boule, K. Othmen, C. Richard, B. Szczepanik, G. Grabner, Phototransformation of halogenoaromatic derivatives in aqueous solution, *Int. J. Photoenergy*. 1 (1999) 49-54.
- [14] S.E. Manahan, *Toxicological chemistry and biochemistry*, CRC Press 2002.
- [15] F.P. Silverman, P.D. Petracek, D.F. Heiman, C.M. Fledderman, P. Warrior, Salicylate activity. 3. Structure relationship to systemic acquired resistance, *J. Agr. Food. Chem.* 53 (2005) 9775-9780.
- [16] T. Reglinski, P. Elmer, J. Taylor, F. Parry, R. Marsden, P. Wood, Suppression of Botrytis bunch rot in Chardonnay grapevines by induction of host resistance and fungal antagonism, *Australas. Plant. Path.* 34 (2005) 481-488.
- [17] T.A. Ternes, R. Hirsch, Occurrence and behavior of X-ray contrast media in sewage facilities and the aquatic environment, *Environ. Sci. Technol.* 34 (2000) 2741-2748.
- [18] L. Xu, R. Yuan, Y. Guo, D. Xiao, Y. Cao, Z. Wang, J. Liu, Sulfate radical-induced degradation of 2, 4, 6-trichlorophenol: a de novo formation of chlorinated compounds, *Chem. Eng. J.* 217 (2013) 169-173.

- [19] H.V. Lutze, S. Bircher, I. Rapp, N. Kerlin, R. Bakkour, M. Geisler, C. von Sonntag, T.C. Schmidt, Degradation of chlorotriazine pesticides by sulfate radicals and the influence of organic matter, *Environ. Sci. Technol.* 49 (2015) 1673-1680.
- [20] O. Brede, S. Kapoor, T. Mukherjee, R. Hermann, S. Naumov, Diphenol radical cations and semiquinone radicals as direct products of the free electron transfer from catechol, resorcinol and hydroquinone to parent solvent radical cations, *PCCP* 4 (2002) 5096-5104.
- [21] M.R. Ganapathi, R. Hermann, S. Naumov, O. Brede, Free electron transfer from several phenols to radical cations of non-polar solvents, *PCCP* 2 (2000) 4947-4955.
- [22] P. Caregnato, P.M. David Gara, G.N. Bosio, M.C. Gonzalez, N. Russo, M.d.C. Michelini, D.O. Mártire, Theoretical and experimental investigation on the oxidation of gallic acid by sulfate radical anions, *J. Phys. Chem. A*. 112 (2008) 1188-1194.
- [23] L. Zhou, M. Sleiman, C. Ferronato, J.-M. Chovelon, P. de Sainte-Claire, C. Richard, Sulfate radical induced degradation of  $\beta$ 2-adrenoceptor agonists salbutamol and terbutaline: Phenoxy radical dependent mechanisms, *Water. Res.* 123 (2017) 715-723.
- [24] R. Tafer, M. Sleiman, A. Boulkamh, C. Richard, Photomineralization of aqueous salicylic acids. Photoproducts characterization and formation of light induced secondary OH precursors (LIS-OH) *Water Research* 106 (2016) 496-506.
- [25] M.J. Frisch, G. Trucks, H. Schlegel, G. Scuseria, M. Robb, J. Cheeseman, G. Scalmani, V. Barone, B. Mennucci, G. Petersson, Gaussian 09, Revision D. 01, Gaussian, Inc.: Wallingford, CT (2009).
- [26] L. Zhou, C. Yan, M. Sleiman, C. Ferronato, J.-M. Chovelon, X. Wang, C. Richard, Sulfate radical induced degradation of  $\beta$ 2-adrenoceptor agonists salbutamol and Terbutaline: Implication of halides, bicarbonate, and natural organic matter, *Chem. Eng. J.* 368 (2019) 252-260.
- [27] A.D. Becke, Becke's three parameter hybrid method using the LYP correlation functional, *J. Chem. Phys.* 98 (1993) 5648-5652.
- [28] A.V. Marenich, C.J. Cramer, D.G. Truhlar, Universal solvation model based on solute electron density and on a continuum model of the solvent defined by the bulk dielectric constant and atomic surface tensions, *J. Phys. Chem. B*. 113 (2009) 6378-6396.

- [29] Y. Wu, A. Bianco, M. Brigante, W. Dong, P. de Sainte-Claire, K. Hanna, G. Mailhot, Sulfate Radical Photogeneration Using Fe-EDDS: Influence of Critical Parameters and Naturally Occurring Scavengers, *Environ. Sci. Technol.* 49 (2015). 14343-14349.
- [30] J. Feitelson, E. Hayon, A. Treinin, Photoionization of phenols in water. Effects of light intensity, oxygen, pH, and temperature, *J. Am. Chem. Soc.* 95 (1973) 1025-1029.
- [31] X. Chen, D.S. Larsen, S.E. Bradforth, I.H. van Stokkum, Broadband spectral probing revealing ultrafast photochemical branching after ultraviolet excitation of the aqueous phenolate anion, *J. Phys. Chem. A.* 115 (2011) 3807-3819.
- [32] D.W. Silverstein, N. Govind, H.J. van Dam, L. Jensen, Simulating One-Photon Absorption and Resonance Raman Scattering Spectra Using Analytical Excited State Energy Gradients within Time-Dependent Density Functional Theory, *J. Chem. Theory. and Comput.* 9 (2013) 5490-5503.
- [33] P.M.D. Gara, G.N. Bosio, M.C. Gonzalez, N. Russo, M. del Carmen Michelini, R.P. Diez, D.O. Mártire, A combined theoretical and experimental study on the oxidation of fulvic acid by the sulfate radical anion, *Photoch. Photobio. Sci.* 8 (2009) 992-997.
- [34] U. Wille, Sulfate Radical Anions ( $\text{SO}_4^{\bullet-}$ ) as Donor of Atomic Oxygen in Anionic Transannular, Self-Terminating, Oxidative Radical Cyclizations, *Org. Lett.* 2 (2000) 3485-3488.
- [35] X. Li, J.W. Cubbage, T.A. Tetzlaff, W.S. Jenks, Photocatalytic degradation of 4-chlorophenol. 1. The hydroquinone pathway, *J. Org. Chem.* 64 (1999) 8509-8524.
- [36] J. Wells, J.E. Ham, A new agent for derivatizing carbonyl species used to investigate limonene ozonolysis, *Atmos. Environ.* 99 (2014) 519-526.
- [37] T. Zhang, Y. Chen, T. Leiknes, Oxidation of Refractory Benzothiazoles with PMS/CuFe<sub>2</sub>O<sub>4</sub>: Kinetics and Transformation Intermediates, *Environ. Sci. Technol.* 50 (2016) 5864-5873.
- [38] Y. Ji, Y. Fan, K. Liu, D. Kong, J. Lu, Thermo activated persulfate oxidation of antibiotic sulfamethoxazole and structurally related compounds, *Water. Res.* 87 (2015) 1-9.
- [39] L. Zhou, Y. Zhang, R. Ying, G. Wang, T. Long, J. Li, Y. Lin, Thermo-activated persulfate oxidation of pesticide chlorpyrifos in aquatic system: kinetic and mechanistic investigations, *Environ. Sci. Pollut. R.* (2017) 1-10.

- [40] Y. Ji, Y. Fan, K. Liu, D. Kong, J. Lu, Thermo activated persulfate oxidation of antibiotic sulfamethoxazole and structurally related compounds, *Water. Res.* 87 (2015) 1-9.
- [41] G.-D. Fang, D.D. Dionysiou, D.-M. Zhou, Y. Wang, X.D. Zhu, J.-X. Fan, L. Cang, Y.J. Wang, Transformation of polychlorinated biphenyls by persulfate at ambient temperature, *Chemosphere.* 90 (2013) 1573-1580.
- [42] Y. Ji, Y. Shi, W. Dong, X. Wen, M. Jiang, J. Lu, Thermo-activated persulfate oxidation system for tetracycline antibiotics degradation in aqueous solution, *Chem. Eng. J.* 298 (2016) 225-233.
- [43] Y. Fan, Y. Ji, D. Kong, J. Lu, Q. Zhou, Kinetic and mechanistic investigations of the degradation of sulfamethazine in heat-activated persulfate oxidation process, *Chem. Eng. J.* 200 (2015) 39-47.
- [44] I. Kolthoff, I. Miller, The chemistry of persulfate. I. The kinetics and mechanism of the decomposition of the persulfate ion in aqueous medium<sup>1</sup>, *J. Am. Chem. Soc.* 73 (1951) 3055-3059.
- [45] C. Liang, H.W. Su, Identification of sulfate and hydroxyl radicals in thermally activated persulfate, *Ind. Eng. Chem. Res.* 48 (2009) 5558-5562.
- [46] C. Zhu, F. Zhu, C. Liu, N. Chen, D. Zhou, G. Fang, J. Gao, Reductive hexachloroethane degradation by S<sub>2</sub>O<sub>8</sub><sup>2-</sup> with thermal activation of persulfate under anaerobic conditions, *Environ. Sci. Technol.* 52 (2018) 8548-8557.
- [47] W. Qin, G. Fang, Y. Wang, D. Zhou, Mechanistic understanding of polychlorinated biphenyls degradation by peroxymonosulfate activated with CuFe<sub>2</sub>O<sub>4</sub> nanoparticles: Key role of superoxide radicals, *Chem. Eng. J.* 348 (2018) 526-534.
- [48] P. Neta, J. Grodkowski, Rate constants for reactions of phenoxy radicals in solution, *J. Phys. Chem. Ref. Data.* 34 (2005) 109-199.
- [49] C. Rice-Evans, N. Miller, G. Paganga, Antioxidant properties of phenolic compounds, *Trends. Plant. Sci.* 2 (1997) 152-159.
- [50] C. Liang, Z.S. Wang, N. Mohanty, Influences of carbonate and chloride ions on persulfate oxidation of trichloroethylene at 20 C, *Sci. Total. Environ.* 370 (2006) 271-277.
- [51] Y. Wang, J. Le Roux, T. Zhang, J.P. Croué, Formation of brominated disinfection byproducts from natural organic matter isolates and model compounds in a sulfate radical-based oxidation process, *Environ. Sci. Technol.* 48 (2014) 14534-14542.

- [52] G.R. Aiken, Chloride interference in the analysis of dissolved organic carbon by the wet oxidation method, *Environ. Sci. Technol.* 26 (1992) 2435-2439.
- [53] J. Liu, X. Zhang, Comparative toxicity of new halophenolic DBPs in chlorinated saline wastewater effluents against a marine alga: Halophenolic DBPs are generally more toxic than haloaliphatic ones, *Water. Res.* 65 (2014) 64-72.
- [54] M. Yang, X. Zhang, Comparative developmental toxicity of new aromatic halogenated DBPs in a chlorinated saline sewage effluent to the marine polychaete *Platynereis dumerilii*, *Environ. Sci. Technol.* 47 (2013) 10868-10876.
- [55] R. Tafer, P. de Sainte- Claire, P. Vicendo, A. Boulkamh, C. Richard, Photochemistry of 5- Halogenosalicylic Acids: Evidence of the Triplet Involvement in the Carbene Formation, *Chem. Select.* (2016) 4704-4712.
- [56] H. Herrmann, A. Reese, R. Zellner, Time-resolved UV/VIS diode array absorption spectroscopy of  $\text{SO}_x^-$  ( $x=3, 4, 5$ ) radical anions in aqueous solution, *J. Mol. Struct.* (1995) 183-186.
- [57] H.V. Lutez, N. Kerlin, T. C. Schmidt, Sulfate radical-based water treatment in presence of chloride: Formation of chlorate, inter-conversion of sulfate radicals into hydroxyl radicals and influence of bicarbonate, *Water Res.* 72 (2015) 349-360.
- [58] B. K. Paul, A. Samanta, N. Guchhait, Deciphering the photophysics of 5-chlorosalicylic acid: evidence for excited-state intramolecular proton transfer, *Photochem. Photobiol. Sci.* 9 (2010) 57-67.
- [59] F. Ghanbari, C. A. Martinez-Huitle, Electrochemical advanced oxidation processes coupled with peroxymonosulfate for the treatment of real washing machine effluent: A comparative study, *J. Electroanal. Chem.* 847 (2019) 113182.
- [60] M Ahamadi, F Ghanbari, Organic dye degradation through peroxymonosulfate catalyzed by reusable graphite felt/ferriferrous oxide: Mechanism and identification of intermediates, *Mater. Res. Bull.* 111(2019), 43-52.

[61] X. Li, M. Zhou, Y. Pan, Enhanced degradation of 2,4-dichlorophenoxyacetic acid by pre-magnetization Fe-C activated persulfate: Influential factors, mechanism and degradation pathway. *J. Hazard. Mater.* 335 (2018) 454-465.

[62] S. Wang, J. Wang, Activation of peroxymonosulfate by sludge-derived biochar for the degradation of triclosan in water and wastewater. *Chem. Eng. J.* 365 (2019) 350-358.